Starting-up strategies for solar thermal fields attending to time and economic criteria: Application of hierarchical control

Juan D. Gil * **Lidia Roca** ** **Manuel Berenguel** *

* *Centro Mixto CIESOL, ceiA3, Universidad de Almería. Ctra. Sacramento s/n, Almería 04120, Spain; {juandiego.gil,beren}@ual.es.*
** *CIEMAT-Plataforma Solar de Almería, Ctra. de Senés s/n, Tabernas 04200, Almería, Spain; lidia.roca@psa.es*

Abstract:
Solar thermal fields are usually coupled to storage tanks to improve the energy dispatchability. In direct configuration and without an auxiliary energy source, the state of the storage tank at the beginning of the operation is very relevant. If the storage device is stratified or discharged in terms of energy, the start-up phase until reaching the desired operating point can take a long time and reduce the benefits. Consequently, this paper presents a two-layer hierarchical controller aimed at reducing the costs and time spent in this operating phase. The upper layer is based on a Nonlinear Model Predictive Control (NMPC) strategy, and the lower one is composed of Proportional Integral Derivative (PID) controllers. The proposed technique was applied to a real facility located at Plataforma Solar de Almería (southest of Spain). Moreover, a comparative simulation study with manual and previous approaches proposed in literature was performed to evidence the important economic and time savings achieved by the application of the developed technique.

Keywords: Solar Energy, Model Predictive Control, PID control, process control.

1. INTRODUCTION

The exhaustion of conventional resources such as fossil fuel, and the prospering concern about climate change, have led to an accelerated search of substitute energy sources. Among the different renewable solutions, solar energy stands out in any sustainable development scenario with high availability of solar irradiance, both to power thermal processes and produce electricity. However, although this technology is industrially implemented worldwide, there is still room for researching and enhancing its performance and operation (Kumar et al., 2018).

One of the main steps towards the improvement of the performance of this technology consisted of its combination with adequate storage devices (Gibb et al., 2018). Taking into account the thermal load or the power block, the storage device, and the solar field, different connection modes can be found in the literature (Biencinto et al., 2014). One of the most used to power thermal loads and especially, in low concentration applications, is the single tank with direct storage (Camacho and Gallego, 2013; Artur et al., 2018). In this configuration, the solar field is directly coupled to the storage tank, and the tank is in charge of delivering the thermal fluid to the load. However, in spite of the great possibilities of improvement that these types of combinations offer to solar thermal technology, the development of optimal operating strategies for its correct use has hardly been addressed in the literature.

Considering the single tank with direct storage configuration, only a few works proposed optimal operating procedures. Berenguel et al. (2005) developed a hierarchical controller tasked with maximizing the electricity production of the plant by optimizing its operation in real-time. Camacho and Gallego (2013) presented a similar control structure but aimed at minimizing the thermal losses in the solar field. Our previous work Gil et al. (2018b) also proposed a hierarchical controller in charge of optimally operating the plant with the objective of maximizing the production of a thermal desalination unit. In summary, the aforementioned works are focused on the operation of these kinds of facilities after the start-up phase. An adequate start-up procedure is essential in these kinds of configurations as if the storage device is widely stratified, or discharged in terms of thermal energy, the transient regime until reaching the operating point can take a long time, which causes a loss of production time, and therefore, of benefits. As stated in Cirre et al. (2009), heuristic-rules are often used in this stage which are proposed according to the storage tank states. Nevertheless, these rules may be ineffective as they do not consider the changing operating conditions to which the plant is subjected due to solar energy behavior.

⋆ This work has been funded by the National R+D+i Plan Project DPI2017-85007-R of the Spanish Ministry of Science, Innovation and Universities and ERDF funds. Juan D. Gil is supported by an FPI Fellowship from the University of Almería. The authors also thank CIEMAT-Plataforma Solar de Almería for facilitating access to its facilities, which were co-funded by the EU Regional Development Funds and the Spanish Ministry of Science and Innovation under project SolarNOVA-I (ICT-CEPU2009-0001).

To the best of our knowledge, only two works deal with the start-up phase of solar thermal fields. López-Álvarez et al. (2018) presented a dynamical offline optimization method to calculate the optimal flow rate that should be applied according to the storage tank states. The objective of that work was to reduce the time spent in this phase trying to achieve full operation of the plant as fast as possible. Nevertheless, the offline calculation method proposed in that work has the same drawback as mentioned above regarding the procedures based on heuristic-rules. A real-time management method was proposed in our previous work Gil et al. (2018a). This management method was based on the use of a two-layer controller. The lower layer, the regulatory one, was tasked with maintaining the main variables involved in the process at the desired setpoints. The upper layer was responsible for calculating the setpoints according to the operating conditions by solving a static optimization problem aimed at maximizing the thermal energy stored in the tank. Note that this objective is similar to the one related to minimizing the start-up phase duration. Although the application of this technique produced satisfactory results, the static decision making that occurs in the upper layer can be improved by using receding horizon strategies.

Motivated by the above literature review, the contributions of this work are two-fold. First, we developed a hierarchical control structure which improves the one presented in Gil et al. (2018a) by using: i) a Practical Nonlinear Model Predictive Control (PNMPC) approach (Plucenio et al., 2007) in the upper layer which includes the dynamical nonlinear models of the facility, and ii) a lower layer with enhanced regulatory control loops. Second, the objective of the controller is not only aimed at reducing the time spent in the start-up phase, but it takes into account a tradeoff between the time and the economic cost associated to the operation of the pump involved in this process, what has not been considered in previously published works. It should be commented that the proposed paper is an extension of Gil et al. (2019) in which only time criteria were taken into account. Note that, the economic savings in this phase could be decisive since the plant is not productive during this period, and therefore, this stage only generates economic losses. To demonstrate the effectiveness of the proposed approach, it was applied to a real demonstrative plant located at Plataforma Solar de Almeria (PSA, www.psa.es). Note that the previous works presented in the literature were developed in simulation. In addition, a simulation study comparing the proposed approach with previous and manual start-up strategies is presented evidencing the benefits obtained.

The remainder of the paper is organized as follows. Section 2 describes the plant used as the test environment. Section 3 presents the model of the facility. Section 4 shows the formulation of the hierarchical control technique. Section 5 presents the results obtained with the application of the proposed technique in the real facility and the comparative simulation study. Finally, Section 5 summarizes the main conclusions of the work.

2. TEST CASE FACILITY

The plant used in this work as a real test environment (see Fig. 1) is located at PSA, southest of Spain. This facility has a single tank with direct storage configuration and it is used to power a thermal desalination unit (Zaragoza et al., 2014).

Fig. 1. Real environment at PSA.

As can be observed in Fig. 2, the facility consists of a thermal load (the desalination unit), a storage tank, and a solar thermal field. This field is composed by stationary flat-plate collectors of 2 m^2 of surface area, deployed in two rows with five collectors each. The whole nominal thermal power of the solar field is 7 kW at about 90 °C. Besides, the solar field also includes a cut valve (Valve 2 in Fig. 2) and an expansion vessel which are in charge of rejecting pressure increases and protecting the solar field from the creation of vapor. The solar field is directly coupled to a storage tank with a capacity of 1500 L. Then, this device is connected to the thermal desalination unit through a heat exchanger. The facility is equipped with a Supervisory Control And Data Acquisition (SCADA) system. Table 1 summarizes the main variables monitored and involved in this work. A full description of the facility was presented in Gil et al. (2018b).

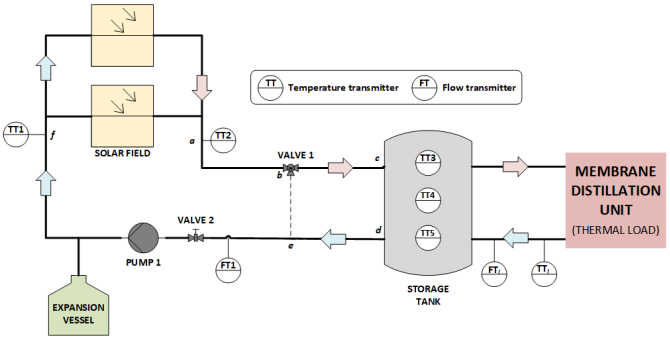

Fig. 2. Layout of the facility.

3. SYSTEM MODELING

This section describes the model of the facility. It should be remarked that most models were already presented and validated in Gil et al. (2019). For this reason, only simplified versions of them are included in this paper due to the lack of space. On the contrary, the new model obtained for the purpose of this work is presented and validated.

Firstly, the temperature at the outlet of the solar field (TT2) is characterized using a lumped-parameter model, which can be described as:

$$\dot{\mathrm{TT2}}(t) = f_1(\mathrm{T}_a(t), \mathrm{I}(t), \mathrm{FT1}(t), \mathrm{TT1}(t)), \qquad (1)$$

Variable	Description	Unit
FT_l	Water flow rate that enters to the tank from the load	(L/min)
F_{P1}	Input frequency percentage of pump 1	(%)
FT1	Water flow rate of solar field	(L/min)
I	Global irradiance at an inclined plane of 35 º	(W/m^2)
P	Total electrical power consumption	(kW)
T_a	Ambient temperature	(ºC)
TT_l	Temperature of the water that enters to the tank from the load	(ºC)
TT1	Temperature at the inlet of the solar field	(ºC)
TT2	Temperature at the outlet of the solar field	(ºC)
TT3	Top tank temperature	(ºC)
TT4	Middel tank temperature	(ºC)
TT5	Bottom tank temperature	(ºC)
V1	Valve 1 position	(%)

Table 1. Variables measured and controlled at the facility.

t is related to the current time, and $f_1(\cdot)$ is a function of its arguments.

Secondly, the temperature at the inlet of the solar field (TT1) is characterized according to the static mass balance of the mix that occurs in the three-way mixing valve:

$$\begin{aligned} \mathrm{TT1}(t) = \mathrm{TT2}(t - t_{r,a-b}) \cdot \frac{\mathrm{V1_m}(t)}{100} \\ +\mathrm{TT5}(t - t_{r,d-e}) \cdot (1 - \frac{\mathrm{V1_m}(t)}{100}), \end{aligned} \quad (2)$$

where $t_{r,a-b}$ and $t_{r,d-e}$ are variable transport delays which will be defined later, and $\mathrm{V1_m}$ is a variable used for modeling the nonlinear behavior of valve 1 relating the location of the valve stem and the portion of mass flow. This was experimentally adjusted by means of polynomials. For positive changes, it can be computed as:

$$\mathrm{V1_m}(t) = f_2(\mathrm{V1}(t)), \quad (3)$$

whereas for the negative ones as:

$$\mathrm{V1_m}(t) = f_3(\mathrm{V1}(t)), \quad (4)$$

where $f_2(\cdot)$ and $f_3(\cdot)$ are polynomial functions.

Thirdly, the temperatures in the storage tank (TT3, TT4 and TT5) are modeled by means of a three-nodes stratified dynamical model:

$$\dot{\mathrm{TT3}}(t) = f_4(\mathrm{TT3}(t), \mathrm{TT2}(t), \mathrm{TT4}(t), T_a(t), \mathrm{FT1}(t)), FT_l(t))), \quad (5)$$

$$\dot{\mathrm{TT4}}(t) = f_5(\mathrm{TT4}(t), \mathrm{TT3}(t), \mathrm{TT5}(t), T_a(t), \mathrm{FT1}(t)), FT_l(t))), \quad (6)$$

$$\dot{\mathrm{TT5}}(t) = f_6(\mathrm{TT5}(t), \mathrm{TT4}(t), \mathrm{TT6}(t), T_a(t), \mathrm{FT1}(t)), FT_l(t))), \quad (7)$$

where $f_4(\cdot)$, $f_5(\cdot)$ and $f_6(\cdot)$ are function of their arguments.

Fourthly, the variable transport delay, produced by the changes of the solar field water flow rate, is modeled in accordance with the ideas proposed in Normey-Rico et al. (1998). Following the proposed procedure, the transport delay ($t_{r,h-i}$) is computed as integer multiples, n_{h-i}, of the sampling time t_s, that is $n_{h-i} \cdot t_s \approx t_{r,h-i}$, where n_{h-i} can be calculated as:

$$n_{h-i} = f_7(v_{h-i}(t)), \quad (8)$$

h and i are related to the points $a, b, ..., f$ of Fig. 2, with $h - i \in \{a-b, b-c, c-d, d-e, e-f\}$, v_{h-i} is the velocity rate (m/s) between points h and i.

Finally, transfer functions experimentally obtained by means of the reaction curve method are used to relate the controlled and the control variables. These functions have the form $p(s) = Y(s)/U(s) = K \cdot e^{-t_d s}/(\tau \cdot s + 1)$ and they are summarized below:

$$p_1(s) = \frac{\mathrm{FT1}(s)}{\mathrm{F_{P1}}(s)} = \frac{0.234}{5s+1} e^{-s}, \; p_2(s) = \frac{\mathrm{TT2}(s)}{\mathrm{FT1}(s)} = \frac{-1.37}{66.62s+1} e^{-16s},$$
$$p_3(s) = \frac{\mathrm{TT1}(s)}{\mathrm{V1}(s)} = \frac{0.102}{43s+1} e^{-79s}. \quad (9)$$

Apart from these transfer functions, which were already presented in Gil et al. (2018b), a new one is calculated for the aim of this work. This transfer function relates the pump 1 input frequency percentage (F_{P1}) with electric power consumption (P):

$$p_4(s) = \frac{\mathrm{P(s)}}{\mathrm{F_{P1}(s)}} = \frac{1.65 \cdot 10^{-3}}{21.58\mathrm{s} + 1}. \quad (10)$$

The validation of this model is presented in Fig. 3. As can be observed, the model provides good results for the whole operating range of F_{P1}. In addition, several valve positions were employed in the test showing that this variable does not affect to this model. In the same way, it can be observed how the movements in the valve hardly affect to the electricity consumption, as the consumption is very low, so it can be assumed that the only device consuming electric power is the pump. The Mean Square Error (MSE) of the validation is 0.014 kW.

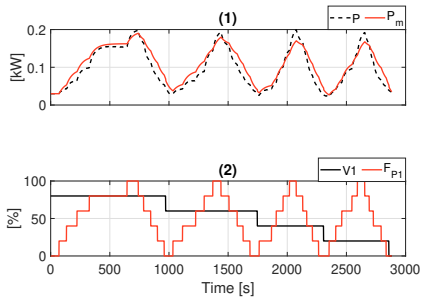

Fig. 3. Validation of the model relating F_{P1} and P. (1) actual electric consumption (P), and electric consumption provided by the model (P_m), and (2) valve 1 aperture (V1) and pump 1 input frequency percentage (F_{P1}).

4. CONTROL SYSTEM FORMULATION

The control system aims to optimally managing the start-up phase of the facility. With this objective, two main issues are taken into account. First, the time spent problem must be minimized. This can be formulated as maximizing the temperature in the upper part of the tank (TT3), see Gil et al. (2018a) for more details. Second, the economic costs associated to this phase must be reduced. This can be proposed as minimizing the electric power consumption (P). The problem is that these two objectives require contrary operating conditions in the solar field pump. Therefore, the upper layer of the proposed hierarchical controller (see Fig. 4) is tasked with calculating a tradeoff solution for these two objectives, which is achieved by using a weighted sum optimization method embedded in the PNMPC controller. The outputs of this layer are the setpoints to be tracked by the upper one. The

selected controlled variables in the regulatory layer are the outlet and inlet temperatures of the solar field, which are controlled by manipulating the two available control variables in the process; the pump 1 input frequency and the valve 1 aperture respectively (see Fig. 4). The selection of TT2 as controlled variable in this kind of systems is natural, since it allows us to keep a suitable outlet of the solar field temperature for loading the tank, i.e. TT2>TT3. Moreover, the TT1 control loop let us establish an adequate inlet temperature in the solar field for loading the tank, in other words, it enables to maintain TT2>TT3. The key of this control loop is that, as TT1 is controlled using the valve aperture, an optimal selection of the setpoint of this variable allows us to gradually load the tank (by gradually opening valve 1 towards the tank during the start-up phase) even with low values of irradiance, thus heating the tank faster than with other operating procedures, helping to minimize the time spent in the start-up procedure.

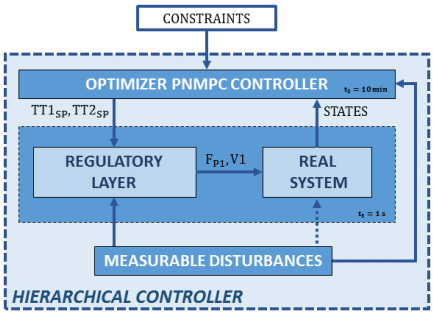

Fig. 4. Schematic diagram of the proposed control architecture.

4.1 Lower layer

As stated before, the lower layer of the hierarchical control architecture is tasked with tracking the references computed by the upper one. In this case, two regulatory loops are used.

To control TT2, a cascade control structure is used. In this control architecture, the slave loop is tasked with controlling the flow rate (FT1) by manipulating the pump input frequency (F_{P1}). The outer loop is aimed at controlling the temperature at the outlet of the solar field (TT2) by manipulating the flow rate (FT1). In addition, a model-based feedforward in series configuration is used to provide the nominal flow rate according to disturbances and operating conditions. The layout of this loop, as well as its configuration, has not been included in this work due to the lack of space, but it was presented in (Gil et al., 2018b).

The main improvement in this regulatory layer (in comparison to the approach presented in Gil et al. (2018a)) is introduced in the TT1 control loop. It can be observed that two main problems must be faced in this loop: i) the dynamic of the process is a delay dominant one (see Eq. (2) and (9)-p_3), and ii) the valve has a nonlinear behaviour (see Eq. (3), (4)). To deal with the first problem, a Filtered Smith Predictor (FSP) (Normey-Rico and Camacho, 2007) controller is chosen as control architecture. The layout of this loop is presented in Fig. 5. To solve the second problem, the fast model of the FSP structure is modified compared to the classical implementation of the FSP controller, in which a linear transfer function is used as a model. This modification consists on including a block implementing the nonlinear model of the valve presented in Eqs. (2), (3) and (4) (note that this was not included in the approach presented in Gil et al. (2018a)). This allows us to modify the gain of the model according to the nonlinear behavior of the valve. Moreover, a low pass filter with a fixed time constant (LFP-2 in Fig. 5) for the whole operating range of the valve is used for fitting the dynamic in the fast model, since no significant changes on it were observed in the experimental tests. Similarly, the nominal delay presented in Eq. (9)-$p_3(s)$ is used to model the delay of the system in the FSP structure. It should be noted that the tuning parameters of the control structure are: 40, 43 and 39.50-s for the characteristic time constants of LPF-1, LPF-2 and LPF-3 respectively, and 14.04 %/°C and 43 s for the proportional gain and integral time of the PI controller. They have been obtained by using the procedure presented in Normey-Rico and Camacho (2007).

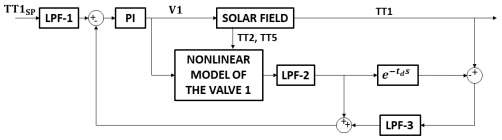

Fig. 5. FSP controlled layout. LPF is a low pass filter, PI is a Proportional Integral controller.

It should be also remarked that the controllers are provided with anti-windup systems taking into account the operational limits of the control variables, which are: 7.5-20 L/min for FT1, 0-100 % for F_{P1}, and 20-80 % for V1.

4.2 Upper layer

The upper layer is based on a Nonlinear Model Predictive Control (NMPC) strategy. Among the different NMPC methodologies presented in the literature, the PNMPC one, which was proposed in Plucenio et al. (2007), is chosen for the purpose of this work. In this technique, the prediction of the output of the process, $\hat{\mathbf{Y}}$, in a given prediction horizon, N, is approximated as a linear function of the future control signals, $\mathbf{\Delta u}$. This can be vectorially computed as:

$$\hat{\mathbf{Y}} \approx \mathbf{f} + \mathbf{G} \cdot \mathbf{\Delta u}, \tag{11}$$

where $\hat{\mathbf{Y}}=[\hat{Y}(t+1|t)...\hat{Y}(t+N|t)]^T$ *, $\mathbf{f}=[\hat{f}(t+1|t)...\hat{f}(t+N|t)]^T$, $\mathbf{\Delta u}=[\Delta u(t|t)...\Delta u(t+N_u-1|t)]^T$, N_u being the control horizon, and $\mathbf{G}$ being the Jacobian matrix $\frac{\partial \hat{\mathbf{Y}}}{\partial \mathbf{\Delta u}}$ computed in the operating point u.

According to the objectives mentioned above for the problem concerning this work, the PNMPC technique is used to compute the predictions of TT3 and P. On the one hand, the prediction of TT3 depends of the two setpoints

* The nomenclature $\hat{z}(t+k|t)$ is related to the value of $\hat{z}$ at discrete instant time $t+k$, computed with the information acquired up to instant t.

of the regulatory layer control loops, $TT1_{SP}$ and $TT2_{SP}$, as both variables influence the behaviour of TT3. Thus, it can be calculated as:

$$\left[\,\hat{\mathbf{Y}}_{\mathbf{TT3}}\,\right] \approx \left[\,\mathbf{f}_{\mathbf{TT3}}\,\right] + \left[\,\mathbf{G_1}\;\mathbf{G_2}\,\right] \cdot \begin{bmatrix} \mathbf{\Delta TT1_{SP}} \\ \mathbf{\Delta TT2_{SP}} \end{bmatrix}, \quad (12)$$

$$\mathbf{G_1} = \frac{\partial \hat{\mathbf{Y}}_{\mathbf{TT3}}}{\partial \mathbf{\Delta TT1_{SP}}}, \mathbf{G_2} = \frac{\partial \hat{\mathbf{Y}}_{\mathbf{TT3}}}{\partial \mathbf{\Delta TT2_{SP}}}. \quad (13)$$

On the other hand, the prediction of P depends only of $TT2_{SP}$, since the pump, which is the only device consuming electricity, is only involved in this control loop. In this way, it can be calculated as:

$$\left[\,\hat{\mathbf{Y}}_{\mathbf{P}}\,\right] \approx \left[\,\mathbf{f}_{\mathbf{P}}\,\right] + \left[\,\mathbf{G_3}\,\right] \cdot \left[\,\mathbf{\Delta TT2_{SP}}\,\right], \quad (14)$$

$$\mathbf{G_3} = \frac{\partial \hat{\mathbf{Y}}_{\mathbf{P}}}{\partial \mathbf{\Delta TT2_{SP}}}. \quad (15)$$

It should be remarked that, in order to add robustness, the integral of the filtered error is added to the predictions following the proposal presented in Plucenio et al. (2007).

Once the predictions are estimated, the control signals are found by solving an optimization problem. In this case, as a tradeoff solution must be obtained due to the presence of two objectives that require contrary operating conditions, the optimization problem is formulated as a weighted sum optimization problem. In addition, as the prediction has a different numerical scale, and also their numerical values change depending on the operating point u, a normalization method is performed at each sampling time, which is given by:

$$m_1 \cdot \hat{\mathrm{Y}}_{\mathrm{TT3}} = m_2 \cdot \hat{\mathrm{Y}}_{\mathrm{P}} = 1, \quad (16)$$

where m_1 and m_2 are scaling factors, and the predictions ($\hat{\mathrm{Y}}_{\mathrm{TT3}}$ and $\hat{\mathrm{Y}}_{\mathrm{P}}$) are evaluated in the operating point u to obtain them. In this way, by redefining $\hat{\mathrm{Y}}^{\mathrm{N}}_{\mathrm{TT3}} = m_1 \cdot \hat{\mathrm{Y}}_{\mathrm{TT3}}$ and $\hat{\mathrm{Y}}^{\mathrm{N}}_{\mathrm{p}} = m_2 \cdot \hat{\mathrm{Y}}_{\mathrm{p}}$, the overall optimization problem can be proposed as:

$$\min_{\Delta \mathrm{TT1}, \Delta \mathrm{TT2}} \mathrm{J} = -\alpha \cdot \left[\sum_{k=1}^{k=N} \hat{\mathrm{Y}}^{\mathrm{N}}_{\mathrm{TT3}}(t+k|t)\right] + \beta \cdot \left[\sum_{k=1}^{k=N} \hat{\mathrm{Y}}^{\mathrm{N}}_{\mathrm{P}}(t+k|t)\right] + \gamma \cdot \left[\sum_{k=1}^{k=N_u} (|\Delta \mathrm{TT1_{SP}}(t+k-1)| + |\Delta \mathrm{TT2_{SP}}(t+k-1)|)\right], \quad (17)$$

Subject to: $\forall\, k \in 1, ..., N_u$

$$\mathrm{TT2}(t+k-1) < 100, \quad (18)$$

$$\mathrm{TT2}(t+k-1) > \mathrm{TT1}(t+k-1), \quad (19)$$

$$\mathrm{TT2}(t+k-1) > \hat{\mathrm{Y}}_{\mathrm{TT3}}(t+k|t), \quad (20)$$

$$\mathrm{TT2_{Min}}(t) < \mathrm{TT2}(t+k-1) < \mathrm{TT2_{Max}}(t), \quad (21)$$

where α, β and $\gamma \in \{0, 1\}$ are tuning parameters of the PNMPC controller. In this way, in the objective function, Eq. (17), the first term is tasked with maximizing the temperature in the upper part of the tank, the second one is aimed at minimizing the electricity consumption, and the third one, penalizes the changes in the control signals, i.e. it is used to avoid abrupt setpoints changes in the regulatory layer. Regarding the constraints, the one in Eq. (18) is used to prevent the creation of vapor in the solar field as the circulating fluid is water. The second and the third ones, Eqs. (19) and (20), are used to ensure the operating constraints related to TT2, which cannot be lower than TT1 and TT3. Finally, the last constraint is also related to TT2, but in this case, it limits the maximum and minimum temperatures, $TT2_{Max}$ and $TT2_{Min}$ respectively, reachable at each sampling time. These limits are calculated by using the solar field model (see Eq. (1)) in the static version. It should be remarked that this way of formulating the multiobjective optimization problem has been chosen since it is more instinctive for the operators of the facility, as they have available two tuning parameters (α and β) to modify the interests of the operation.

5. RESULTS AND DISCUSSION

This section presents the results obtained with the application of the developed control method. First, the results during a day operating the real facility are presented. Second, a comparative simulation study with manual and previous approaches are shown. To perform the aforementioned tests, the sampling time of the lower layer was fixed at 1 s, whereas a sampling time of 10 min was used in the upper one. These values were selected considering the time constant of the main variables involved in each layer. The control and prediction horizons in the PNMPC technique were fixed at 3 and 6 respectively, following traditional recommendations in these kinds of controllers $N_u \ll N$, and after performing several simulations until reaching the desired closed-loop behavior. Similarly, γ was fixed at 0.01 which prevents the references of the lower layer from suffering abrupt changes while not compromising the true objectives of the optimization problem. On the contrary, α and β were chosen depending on the interests of the operation, as will be shown in the following subsections.

5.1 Experimental test

The experimental test was performed on the day of 24 September 2019. In this test, α and β were fixed at 0.5. Note that with these values, both objectives have the same importance on the optimization problem. The results of the test are presented in Fig. 6. As can be seen, the operation started at 9.35 h. This was calculated automatically by the algorithm, by using the method presented in Gil et al. (2018a) in which a static version of the model presented in Eq. (1) is employed to calculate the level of irradiance that allows starting the solar field to heat the tank. In this case, the level was 402.30 $\mathrm{W/m^2}$. When the solar field was turned on, a previous phase before started the hierarchical controller was performed. During this phase, the fluid was circulated only through the solar field until TT2 reached TT3 (see Fig. 6-(2)). This procedure was employed to prevent turning on the automatic operation during the temperature transients caused by the cold fluid inside the pipes at the beginning of the day. In this way, the controller was turned on at 10.09 h.

It should be commented that the expansion vessel of the facility presented an anomalous operating behavior. Note that, this is an exception that occurs only in this plant. This behavior can be seen in Fig. 6-(2) and (3) around instant time 10.09 h, when the controller was turned on. At that moment, the controller introduced a positive step in $TT2_{SP}$. This caused the flow rate to decrease, producing a drastic drop in TT1. This phenomenon was tried to model,

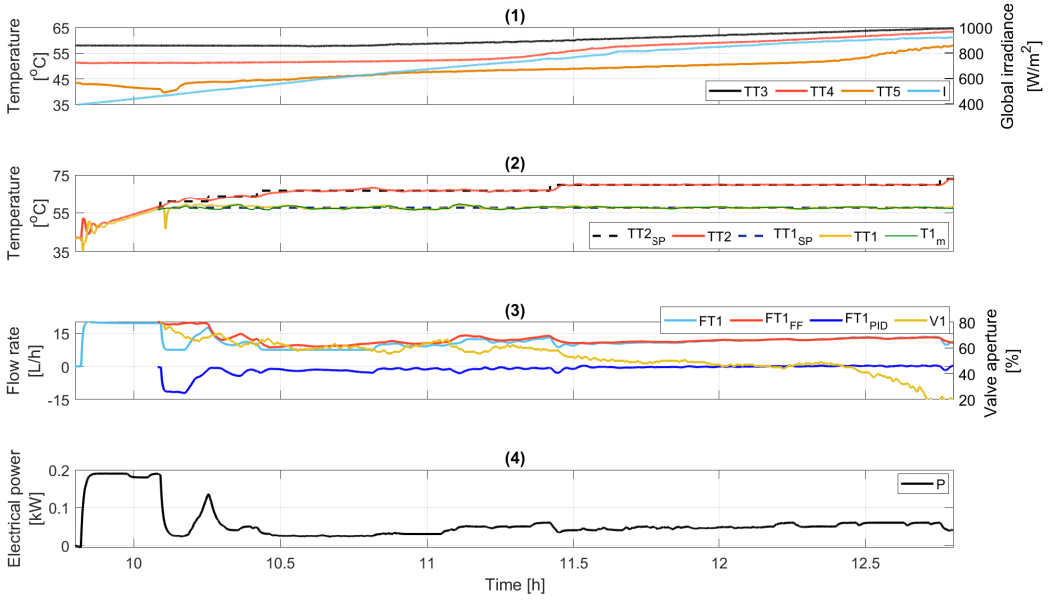

Fig. 6. Experimental test. (1) Temperatures in the tank (TT3, TT4 and TT5) and global irradiance (I), (2) Outlet and inlet temperatures of the solar field (TT2 and TT1), their setpoints ($TT2_{SP}$ and $TT1_{SP}$), and the estimated value for TT1 ($TT1_m$), (3) water flow rate (FT1), feedforward and PID controller signals ($FT1_{FF}$ and $FT1_{PID}$) and valve aperture (V1), and (4) electric consumption (P).

but it was impossible as the temperature decrease has no recognizable sequences. Thus, several open-loop tests were performed to estimate the duration of this effect and the ramp variations in the flow rate which cause the temperature drop. In this way, a decision-maker that checks the changes in the flow rate at each sampling time was implemented. This block decided if the control loop of TT1 is fed back with the real temperature (TT1) or with an estimation computed with the model presented in Eq. (2). This estimation corresponds to $TT1_m$ in Fig. 6-(2).

Regarding the automatic operation, at the first sampling time, the upper layer of the controller fixed the setpoints for TT1 and TT2 in 57.4 and 60.95 °C respectively (see Fig. 6-(2)). To track these references, the lower layer decreased the water flow rate, and, as the temperature at the outlet of the solar field increased, valve 1 began to open to use cold fluid from the lower part of the tank to keep the reference in TT1 Fig. 6-(3)). Note also that, hot fluid began to enter the upper part of the tank. It should be remarked that in this test, the tank was highly stratified, the temperature in the lower part at the beginning of the operation was 44.15 °C whereas in the upper part 57.40 °C. Then, around instant time 10.55 h the upper layer introduced another positive step in $TT2_{SP}$ whereas $TT1_{SP}$ was kept constant (see Fig. 6-(2)). In general terms, the same procedure was repeated several times (see instant times 10.80 and 11.45 h in Fig. 6-(2)). By doing this, the controller achieved that the pump worked around the middle of its operating range, thus decreasing the electrical power consumption (see Fig. 6-(4)), and that the valve 1 gradually opened towards the tank, thus heating it. Consequently, the stratification in the tank decreased (see Fig. 6-(1)), and the temperature in the upper tank increased, so that, at instant time 12.75 h, it reached 65 °C which is the reference for turning on the thermal load of the facility.

5.2 Comparative simulation study

To evidence the benefits obtained with the proposed operating strategy, a comparative simulation study was carried out. For this test, real meteorological data from PSA on the day 9 March, 2017 were used. The comparison was performed with the previous approach presented in Gil et al. (2018a) and with a manual one. It is worth noting that, the strategy proposed in López-Álvarez et al. (2018) was developed to be used only in two tank with direct storage configurations, and consequently, it cannot be adjusted to the plant used in this work. For this reason, it has not been included in the comparison. For the tests, the tank temperatures were fixed at TT3 = 58.50, TT4 = 52.60 and TT5=49.40 °C as in (Gil et al., 2019).

The manual operation was performed as follows: i) when the irradiance value reached 500 W/m^2 the solar field pump was activated, afterward, ii) the fluid was circulated only through the solar field until up to reach 80 °C, with FT1 maintained at its minimum operating range, and finally, iii) valve 1 was opened and the fluid, operated at its maximum range, was flowed to the tank until reaching the desired operating temperature. It can be observed that this is a typical rule-based operation in these kinds of systems (Cirre et al., 2009).

The results are presented in Table 2. The two metrics used to evaluate them are: i) the time spent in reaching 65 °C in the upper part of the tank from the beginning of the simulation, and ii) the total electricity costs related to the solar field pump operation, which were calculated as the total electricity consumption of pump 1 multiplied by the standard cost of electricity in Spain (0.12 €/kWh).

As can be seen in Table 2, three different simulations were performed with the method proposed in this paper. The differences between them were the values for α and β. In the first one, proposed approach 1 in Table 2, the values for α and β were 0.8 and 0.2 respectively. In this way, the optimization problem of the upper layer paid more attention to maximize TT3 than to minimize electric consumption. In the second case, proposed approach 2 in Table 2, both parameters were fixed at 0.5, thus balancing the importance of the two objectives in the optimization problem. In the third test, α and β were fixed at 0.2 and 0.8 respectively, thus giving more importance to minimize the electric consumption. It can be observed how by using the proposed approach with configuration 1, the time was reduced up to 22.5 and 7 %, and the costs up to 25 and 14 % in comparison to the manual and previous procedures respectively. It is worth noting that, in this case, although both metrics were improved, the savings in time were more significant due to the value of α and β. In addition, it should be commented that the results in time improved those obtained with the strategy presented in Gil et al. (2018a) thanks to the use of a receding horizon strategy in the upper layer. In the second configuration of the algorithm, proposed approach 2 in Table 2, the time was reduced around 20 and 3 % while the costs around 35 and 25 % concerning the manual and previous approaches. In the last configuration, the costs were considerably reduced, 43 and 35 % compared to the manual and previous operating strategies respectively. On the contrary, the time was improved with respect to the manual procedure around 17 %.

	Time [min]	Costs [€]
Manual procedure	165.26	0.049
Gil et al. (2018a)	137.11	0.043
Proposed approach 1	128.02	0.037
Proposed approach 2	133.02	0.032
Proposed approach 3	137.36	0.028

Table 2. Comparison of results.

6. CONCLUSIONS

This paper addressed the problem associated with the start-up phase of solar thermal fields with direct storage. For this aim, a hierarchical controller composed of two layers is proposed. The upper one is based on an NMPC technique including a weighted sum optimization problem proposed to minimize the time and the costs of this operating phase. The outputs of this layer are the setpoints to be tracked by the lower one, which is based on regulatory controllers. The proposed strategy was applied to a real plant located at PSA. In addition, a comparative simulation study with other operating strategies was performed.

The results obtained show how the proposed strategy is suitable for managing the start-up phase of these kinds of facilities, improving the results obtained by using a manual strategy based on heuristic rules and a previous approach proposed in the literature. Depending on the configuration of the weighted sum method included in the upper layer, the costs can be reduced up to 43 and 35 % with respect to the aforementioned strategies, whereas the time can be reduced around 22.5 and 7 %. These improvements could be very relevant at industrial-scale.

REFERENCES

Artur, C., Neves, D., Cuamba, B.C., and Leão, A.J. (2018). Comparison of two dynamic approaches to modelling solar thermal systems for domestic hot water. *Sustainable Energy Technologies and Assessments*, 30, 292–303.

Berenguel, M., Cirre, C.M., Klempous, R., Maciejewski, H., Nikodem, M., Nikodem, J., Rudas, I., and Valenzuela, L. (2005). Hierarchical control of a distributed solar collector field. In *International Conference on Computer Aided Systems Theory*, 614–620. Springer.

Biencinto, M., Bayón, R., Rojas, E., and González, L. (2014). Simulation and assessment of operation strategies for solar thermal power plants with a thermocline storage tank. *Solar Energy*, 103, 456–472.

Camacho, E. and Gallego, A. (2013). Optimal operation in solar trough plants: A case study. *Solar Energy*, 95, 106–117.

Cirre, C.M., Berenguel, M., Valenzuela, L., and Klempous, R. (2009). Reference governor optimization and control of a distributed solar collector field. *European Journal of Operational Research*, 193(3), 709–717.

Gibb, D., Johnson, M., Romaní, J., Gasia, J., Cabeza, L.F., and Seitz, A. (2018). Process integration of thermal energy storage systems–evaluation methodology and case studies. *Applied Energy*, 230, 750–760.

Gil, J.D., Roca, L., Berenguel, M., and Guzmán, J.L. (2018a). A multivariable controller for the start-up procedure of a solar membrane distillation facility. *IFAC-PapersOnLine*, 51(4), 376–381.

Gil, J.D., Roca, L., Ruiz-Aguirre, A., Zaragoza, G., and Berenguel, M. (2018b). Optimal operation of a solar membrane distillation pilot plant via nonlinear model predictive control. *Computers & Chemical Engineering*, 109, 151–165.

Gil, J.D., Roca, L., Zaragoza, G., Normey-Rico, J., and Berenguel, M. (2019). Hierarchical control for the start-up procedure of solar thermal fields with direct storage. *Control Engineering Practice*.

Kumar, A., Prakash, O., and Dube, A. (2018). A review on technology and promotional initiatives for concentrated solar power in world. *International Journal of Ambient Energy*, 39(3), 297–316.

López-Álvarez, M., Flores-Tlacuahuac, A., Ricardez-Sandoval, L., and Rivera-Solorio, C. (2018). Optimal start-up policies for a solar thermal power plant. *Industrial & Engineering Chemistry Research*, 57(3), 1026–1038.

Normey-Rico, J.E., Bordons, C., Berenguel, M., and Camacho, E.F. (1998). A robust adaptive dead-time compensator with application to a solar collector field. *IFAC Proceedings Volumes*, 31(19), 93–98.

Normey-Rico, J.E. and Camacho, E.F. (2007). *Control of dead-time processes*. Springer Science & Business Media.

Plucenio, A., Pagano, D., Bruciapaglia, A., and Normey-Rico, J. (2007). A practical approach to predictive control for nonlinear processes. *IFAC Proceedings Volumes*, 40(12), 210–215.

Zaragoza, G., Ruiz-Aguirre, A., and Guillén-Burrieza, E. (2014). Efficiency in the use of solar thermal energy of small membrane desalination systems for decentralized water production. *Applied Energy*, 130, 491–499.